2010

Tracking chemical processing pathways in combinatorial polymer libraries via data mining

Scott Broderick
Iowa State University, srbroder@iastate.edu

Joseph R. Nowers
3M Corporation

Balaji Narasimhan
Iowa State University, nbalaji@iastate.edu

See next page for additional authors

Tracking Chemical Processing Pathways in Combinatorial Polymer Libraries via Data Mining

Scott R. Broderick,[†,‡] Joseph R. Nowers,[§,||] Balaji Narasimhan,[‡,§] and Krishna Rajan*[,†,‡]

Department of Materials Science and Engineering, Institute for Combinatorial Discovery, and Department of Chemical and Biological Engineering, Iowa State University, Ames, Iowa 50011, and 3M Corporation, 900 Dayton Avenue, Ames, Iowa 50010

Received September 15, 2009

Changes in the molecular structure and composition of interpenetrating polymer networks (IPNs) can be used to tailor their properties. While the properties of IPNs are typically different than polymer blends, a clear understanding of the impact of changing polymerization sequence on the physical properties and the corresponding molecular bonding is needed. To address this issue, a data mining approach is used to identify the change with polymerization sequence of tensile and rheological properties of acrylate-epoxy IPNs. The experimental approach used to study the molecular structure is high throughput Fourier transform infrared (FTIR) spectroscopy. Analysis of the FTIR spectra of IPNs synthesized with different polymerization sequences leads to an understanding of the molecular bonding responsible for the tensile and rheological properties. From the interpretation of the wavenumber bands and associated molecular bonds, we find that the polymerization sequence most affects hydrogen bonding and aromatic ring bond energies. This work defines the relationships between chemistry, structure, processing, and properties of the IPN samples.

1. Introduction

Combinatorial experiments aim to create large amounts of data and information, which results in challenges in searching the data to find the "hidden" information.[1,2] Most studies of combinatorial libraries focus on the results after the experiment is complete. However, it is equally important to understand the pathway or steps achieved before a particular chemical combination with desired characteristics is formed, from which one can glean information on mechanisms associated with the formation of the target chemistry. In this paper we demonstrate how data mining[3] integrated into the screening of structural data from combinatorial polymer libraries can be used to extract information about the "pathway" of developing targeted characteristic information that otherwise would be missed by simple inspection of screening data. By coupling informatics with high throughput screening data we show how we can rapidly indentify the impact of polymerization sequence on molecular bonding and physical properties of interpenetrating polymer networks (IPNs).

The properties of acrylate-epoxy IPNs have been previously analyzed using data mining, specifically principal component analysis (PCA).[2,4] In those studies, the primary focus was on rheological and tensile properties of the IPNs, with only the conversion of the monomers to polymers as determined by Fourier transform infrared (FTIR) spectroscopy considered and correlated to other properties. The majority of the FTIR spectra was ignored. FTIR spectra are a rich source of information as has been shown before with polyanhydrides.[5] This work continues both of these prior analyses by applying the methodologies we developed for analyzing FTIR spectra of polyanhydrides to the IPN samples, where the IPN samples contain different amounts of epoxy and acrylate. These two monomers have different polymerization mechanisms, and the properties of the IPNs are a strong function of the polymerization sequence of the co-monomers.[6]

The properties of IPNs arise from a permanent entanglement between the polymer networks, and in "ideal" IPNs there are no chemical bonds between the polymers.[7−9] IPNs typically have material properties that are different when compared with the homopolymers or blends of polymers. The structure−property relationships of the IPNs can be complicated by phase separation,[10] which depends on the thermodynamic compatibility of the polymers and the reaction kinetics of the polymerization, as the pre-existence of one polymer network can affect the polymerization rate of the second polymer.[11] In this work, the IPNs were synthesized using a photoinitiated free radical polymerization of a diacrylate and a thermally initiated cationic difunctional epoxy polymerization. The polymerization sequence was varied from photoinitiated first to thermally initiated first, thereby changing the polymerization order from acrylate first to epoxy first.

Data mining is employed because we want to quantify the change in properties due to polymerization sequence and

* To whom correspondence should be addressed. E-mail: krajan@iastate.edu. Phone: 515-294-2670. Fax: 515-294-5444.
† Department of Materials Science, Iowa State University.
‡ Institute for Combinatorial Discovery, Iowa State University.
§ Department of Chemical and Biological Engineering, Iowa State University.
|| 3M Corporation.

10.1021/cc900145d
Published on Web 12/23/2009

identify the bonding responsible for the different properties. In this work, the entire FTIR spectra composed of nearly two thousand data points is analyzed, in addition to the 40 properties from tensile and rheometry experiments. All of these data types exist for multiple samples at each of the eight compositions and polymerization sequence combinations used. PCA is the data mining method employed here because it reduces data dimensionality by redefining the axes so that they correspond with the directions of most variance, where these new axes or principal components (PCs) correspond with the eigenvectors of the original data's covariance matrix.[12−14] While as many PCs exist as dimensions of the original data, typically a few PCs are sufficient to capture the majority of the system's information. By converting the data into the dimensionally reduced PCA space, we can more easily differentiate the differences due to changing composition versus changing polymerization sequence, with the differences clearly aligned with the new axes. The input data set is decomposed into two matrices of interest: scores and loadings. The loadings matrix defines the new axes of the dimensionally reduced data set, while the scores matrix describes the samples in the PC space. Numerous examples of the application of data mining for materials problems exists in the literature.[15−22] However, the use of a multivariate analysis with polymer systems has been more limited.[23−27] With PCA, the most important features of the FTIR spectra can be identified, and the peak shifts and non-symmetries in the peaks between the samples can be quickly determined. We can identify which wavenumbers correspond most closely with the composition of the IPNs and which are most changed because of the polymerization sequence. While multivariate analyses of spectral data have previously been attempted,[28−31] the uniqueness of the work presented here is in the type of system studied and the level of analysis presented.

2. Experimental Section

2.1. Materials and Conversion by FTIR. IPNs were synthesized using a photoinitiated free radical polymerization of a diacrylate and a thermally initiated cationic difunctional epoxy polymerization. The materials used for the acrylate polymerization were poly(ethylene glycol) 200 diacrylate (SR-259, Sartomer, Exton, PA) and free radical initiator α,α-dimethoxy-α-phenylacetophenone (Irgacure 651, Ciba Specialty Chemicals, Basel, Switzerland). The materials used for the epoxy polymerization were a multifunctional epoxy, bisphenol A-epichlorohydrin epoxy resin (EPSON 828, Resolution Performance Products, Houston, TX), and a proprietary thermal activated cationic catalyst, ammonium antimony hexafluoride (XC-7231, King Industries, Norwalk, CT). The chemical structures are shown in Figure 1.

The photoinitiator and catalyst were added at a ratio of 1% to the base resin. The photopolymerization was performed by passing the samples on a conveyer under a high intensity UV light source multiple times, while the thermal polymerization followed a thermal cycle of 1 h at 100 °C, 2 h at 120 °C, and 2 h at 160 °C in a laboratory oven. An FTIR spectrophotometer with diamond ATR (Thermo Nicolet, Waltham, MA) was used to measure IR absorption.

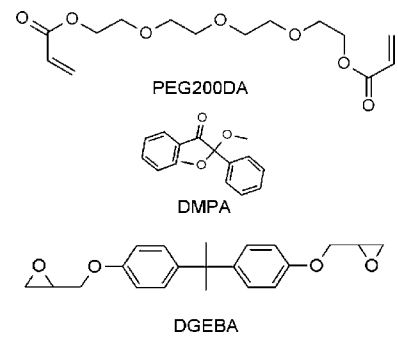

Figure 1. Chemical structures of the acrylate, polyethylene glycol 200 diacrylate (PEG200DA), SR-259; the photoinitiator, α,α-dimethoxy-α-phenylacetophenone (DMPA), Irgacure 651; and the epoxy, diglycidal ether of bisphenol A (DGEBA), Epon 828.

Two sets of IPN samples for measuring physical properties, one set rectangular in shape and the other dog-bone shaped, were prepared with varying composition and with different reaction sequences. The rectangular shaped samples were used for rheological measurements, and the dog-bone shaped samples for evaluation of tensile properties and hardness. In addition, small sections of the samples were evaluated for conversion and residual heats of reaction using attenuated total reflectance FTIR spectroscopy, photo differential scanning calorimetry (pDSC), and modulated differential scanning calorimetry (mDSC). A flowchart of the evaluation techniques with example spectra is shown in Figure 2, with a full description of the methods and equipment used to measure the properties described elsewhere.[6]

2.2. Data Description. The primary data set used in this work contained FTIR spectra for eight different sample types composed of epoxy and acrylate: 25, 50, 75, and 100% acrylate with acrylate reacted prior to epoxy, and 0, 25, 50, and 75% acrylate with epoxy reacted first. The data set was organized as shown in Figure 3, where the descriptors include every wavenumber from the FTIR spectra at 4 cm^{-1} intervals that are otherwise continuous and not discrete. The total number of descriptors used was 1868, with the values in the data set being the absorbances at each wavenumber. The data was not scaled as all units are identical, and larger impact should be given to the larger differences between high intensity peaks. For each polymerization sequence and composition pair, several samples were created, and FTIR analysis was performed on each to minimize and estimate the error. In the PCA analysis, any abnormalities in a particular sample were easily identified by further examining the outliers. For all of the composition-polymerization sequence pairs, multiple spectra exist, resulting in the data set actually including 17 samples.

The samples differ in two major ways: composition and polymerization sequence. An analysis of FTIR spectra by visual inspection or by peak identification can be useful in identifying some differences between samples at a qualitative level, and then attributing these differences to either a change in composition or polymerization sequence. However, too many data values exist to perform a complete analysis of the entire spectra in an efficient manner. The most common strategy is to examine only the wavenumbers that are known to correspond to reactive moieties, while vast regions of the spectra are typically ignored. In some cases reactive sites

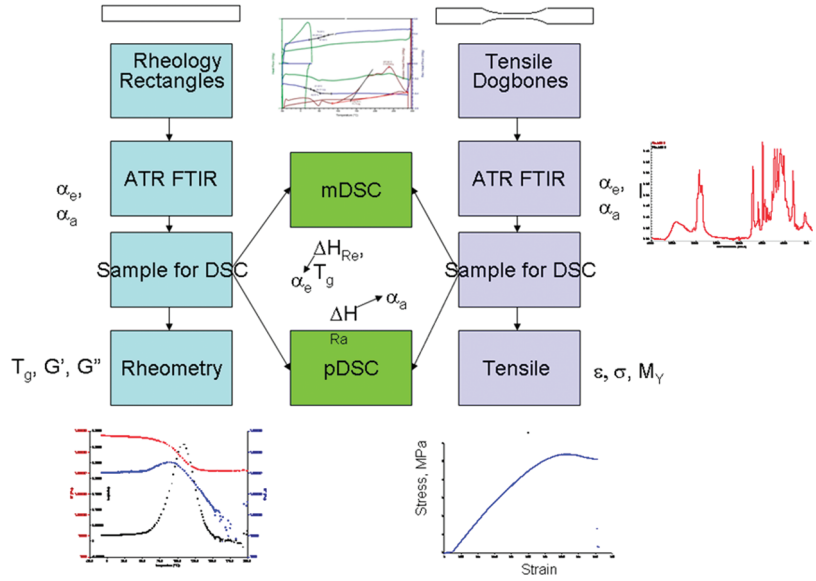

Figure 2. Flowchart and sample spectra of evaluation techniques applied to combinatorial samples created simultaneously from batteries of varying composition. Some of the properties and parameters determined by each technique are indicated in the chart.

can have absorbances at multiple wavenumbers, and traditional analysis of these multiple wavenumbers can lead to conflicting conclusions. Using a multivariate analysis on the entire spectra, a complete analysis of the data can be performed and differences between samples can be attributed to composition or polymerization sequence.

The other data set considered in this work contains values of the measured physical properties, from experimental results on rheological and tensile testing. This data set also contains information on conversion and residual reactions, as well as information about the samples. The compositions and polymerization sequences are the same as in the FTIR data set, with three to seven samples tested for each sample type. The data set contained a total of 24 samples and 40 parameters, with the parameters defined in the appendix.

3. Results

3.1. Analysis of Physical Properties. The data set composed of rheological and tensile measurements was analyzed to explore the impact of polymerization sequence on the physical characteristics of the IPN samples. The data was normalized by first mean centering each descriptor and dividing each value by the standard deviation for that particular descriptor. This results in each set of descriptor values having a mean of zero and a unit variance so that no impact because of different units of descriptors occurs. Figure 4 shows the scores plot, with each point representing the average scores value of the samples at the particular set of conditions, and a loadings plot from the analysis of this data set, with the property labels in the loadings plot defined in the appendix. The percent labeled on the axes corresponded to the amount of variance of the total data set captured by the respective axes. The two reaction sequences are labeled as "A" (acrylate polymerized first) and "E" (epoxy polymerized first). In Figure 4, the differences between polymerization sequence can be clearly observed, with PC1 differentiating the two sequences with sequence A having a negative PC1 value and sequence E having a positive PC1 value, while PC2 captures the differences due to composition, as the PC2 value decreases with increasing acrylate content.

Having identified the physical meaning of the axes, the relationships between composition and polymerization sequence and the rheological/tensile properties can be identified because the scores and loadings plots have the same axes. Therefore, the interpretation of PC1 capturing differences due to polymerization sequence and PC2 capturing differences due to composition was applied to the loadings plot, with the interpretations listed in Table 1. Understanding what the axes represent in Figure 4 allows for tailoring of the IPNs for specific properties. For example, the storage modulus (G′) has a significant negative PC1 value and almost no PC2 value, meaning that changing the acrylate/epoxy composition has minimal effect on G′, while polymerizing acrylate prior to epoxy increases G′ and polymerizing epoxy first decreases G′. As another example, the loss modulus (G″) has a negative PC2 value but minimal PC1 value. Therefore, increasing acrylate composition increases G″ and increasing epoxy percent decreases G″, while changing the order of polymerization has little effect. This analysis can be carried out for all 40 properties so that the relationships between composition, polymerization sequence, and mechanical properties can be identified beyond what is possible without data mining.

The ability to quantify changes in properties such as G′ and G″ because of composition and reaction sequence is very useful in IPN design. Additionally, these results identify the trade-offs needed to improve a particular property. In addition to showing the correlations between the descriptors, the loadings plot shows which properties have the largest effect on the scores plot, as the properties with large magnitudes in PC values have more relevance in determining the PC values of the scores plot. This approach defines chemistry-processing-property relationships for the IPN samples, while the next section relates chemistry and processing with structure.

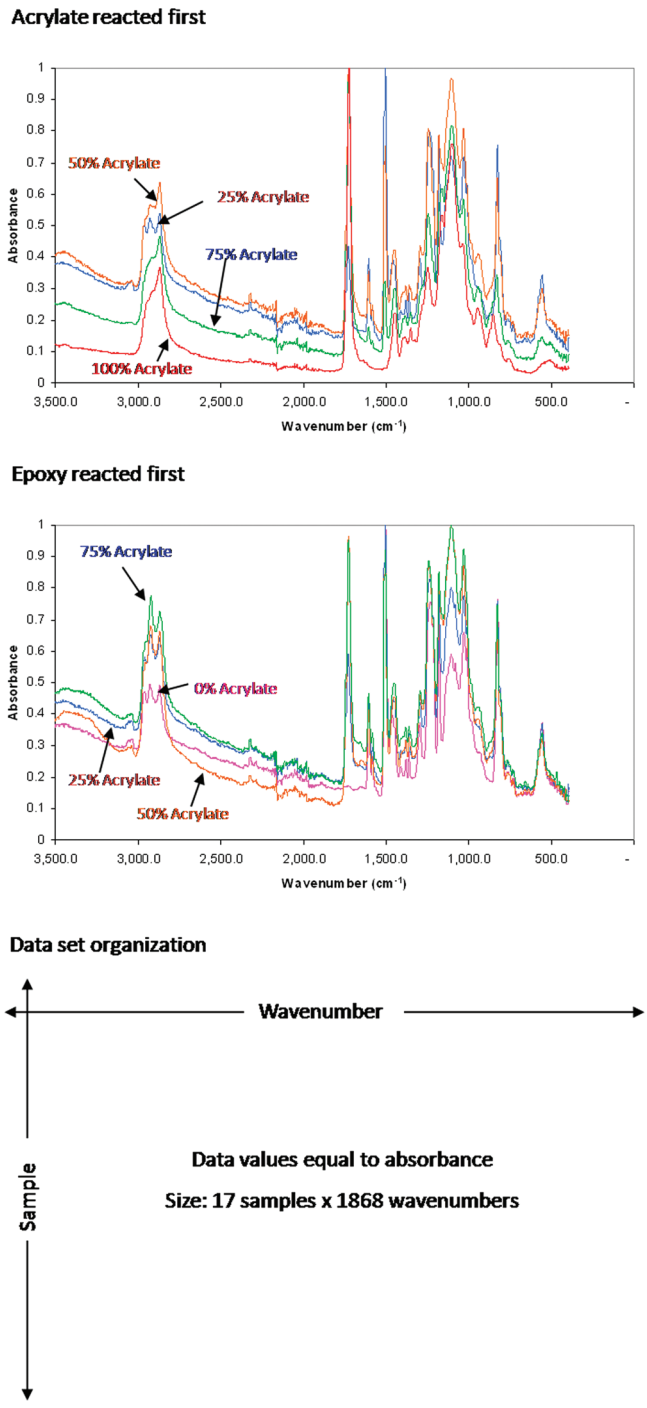

Figure 3. Data set organization for the FTIR spectra of samples with varying compositions and polymerization sequences. Differences clearly exist because of both effects, but quantifying the degree of change due to each effect is difficult because the impact of changing composition is not consistent between polymerization sequences, and likewise the impact of changing polymerization sequence is not consistent between compositions.

3.2. Analysis of FTIR Spectra. We analyzed the FTIR spectra to identify the nature of the molecular bonding responsible for the change in properties with changing polymerization sequence. With the identification of these bonding characteristics, we can then fully develop structure-chemistry-processing-property relationships. Scores and loadings plots of the PC analysis of the FTIR data is shown in Figure 5. As with the analysis of physical properties, the axes can be interpreted in terms of composition and polymerization sequence. In this case PC1 is related to composition and PC2 is related to polymerization sequence. As the PC1 value increases, the acrylate composition increases for both polymerization sequences, while the differences between reaction sequences are captured by PC2.

PC1 describes 77.6% of the variance in the data, while PC2 describes 17.2% of the variance, and thus using only two dimensions instead of the initial 1868 dimensions we are able to capture 94.8% of the variance existing in all of the spectra. On the basis of the ratio between PC1 and PC2, it is found that compositional effects as related to FTIR spectra (molecular bonding) are approximately four times more significant than polymerization sequence effects for the data analyzed.

Table 2 shows how a single PCA plot can be used to condense the data contained in many spectra into information that more fully describes the system. For example, based on the distance from the origin the relative variation in absorbance at a specific wavenumber can be used to describe the system, while the width and symmetry of a loop describes the change in peak heights and wavenumbers. A graphical representation of this interpretation is presented in Figure 6, where the impact due to composition versus polymerization sequence is determined by the trajectory of the loops. This figure shows a loop with a trajectory along both PC1 and PC2, indicating that this peak changes with both composition and polymerization sequence. Conversely, the loadings plot displays the peak at 1724 cm^{-1} (associated with the C═O stretch in the acrylate) primarily along PC1, meaning this peak changes with changing composition but not with polymerization sequence. This result demonstrates an approach for identifying relationships between structure, processing, and chemistry.

4. Discussion

By analyzing physical properties, we were able to develop chemistry-processing-property relationships by quantifying the change in properties as a function of IPN composition and polymerization sequence. Additionally, the analysis of the FTIR spectra led to the development of structure-chemistry-processing relationships, as the relationships between molecular bonding with composition and polymerization sequence were identified. This information leads to the identification of structure-chemistry-processing-property relationships because we have identified how properties change with composition and polymerization sequence, and identified the molecular bonding responsible for the change in properties. In this section, we discuss the specific change in molecular bonding with different polymerization sequence that was identified through the analysis of FTIR spectra. Table 3 lists the wavenumbers where peaks in the FTIR spectra exist and wavenumbers at loop apexes identified from the loadings plot. The molecular bonds, associated monomers, and whether the bond is changed during polymerization are listed in the table.

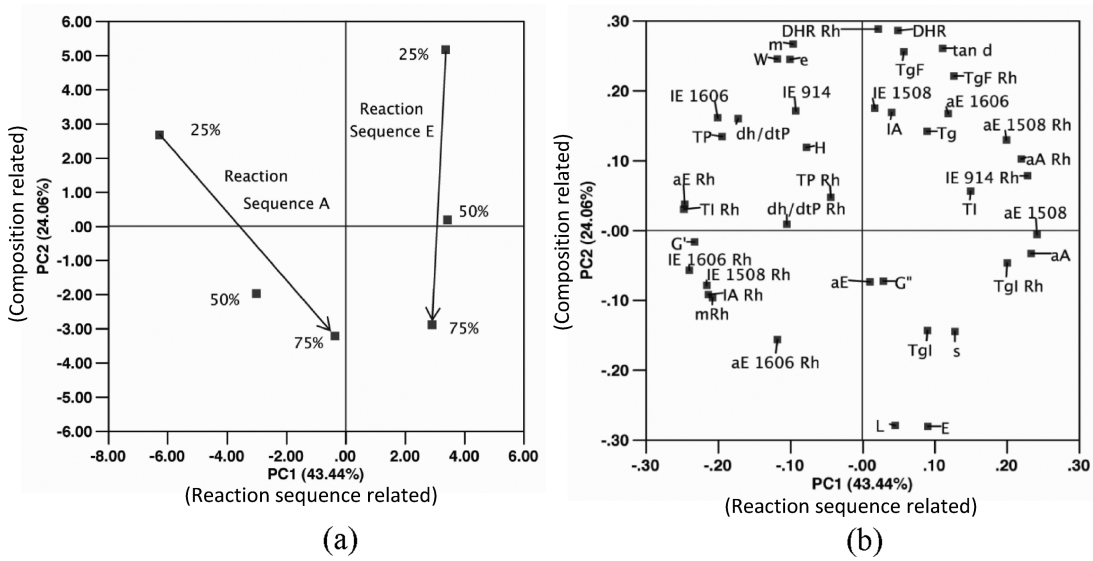

Figure 4. (a) Scores plot of analysis primarily consisting of tensile and rheological properties. On the basis of the trends of the values, PC1 is identified as capturing differences due to reaction sequence, with +PC1 being associated with epoxy polymerized first and -PC1 being associated with acrylate being polymerized first. Likewise, PC2 captures differences due to composition, with increasing acrylate content leading to more negative PC2 value. (b) Loadings plot of the analysis, with the same axes as the scores plot. Having identified the meaning of the axes, the relationship between processing, composition and properties is clearly defined.

Table 1. Relationship between Properties, Composition and Processing, As Described by Figure 4

compositional effect	reaction sequence effect	impacted properties
increase with acrylate	none	L, G″, aE
increase with acrylate	increase with epoxy first	s, E, TgI
increase with acrylate	increase with acrylate first	m Rh, IA Rh, IE1508 Rh, aE1606 Rh
increase with epoxy	none	m, w, e, TgF, IA, DHR, DHR Rh, IE1508
increase with epoxy	increase with epoxy first	tan d, Tg, TgF Rh, aA Rh, TI, aE1606, aE1508 Rh, IE914 Rh
increase with epoxy	increase with acrylate first	H, dh/dtP, TP, TP Rh, IE914, IE1606
none	increase with epoxy first	TgI Rh, aA, aE1508
none	increase with acrylate first	G′, TI Rh, aE Rh, dh/dtP Rh, IE1606 Rh

The bonds that participate in the polymerization of the acrylate or epoxy monomers are indicated with a "yes" in the reactive column in Table 3. The large differences in the spectra as indicated by the loadings plot are not at these reactive sites, but in areas that are typically viewed as "less interesting." Therefore, using PCA we have identified the peaks that most fully differentiate the samples, which would be ignored otherwise. None of the reactive bond regions figure as prominently in the loadings plot although this finding is somewhat expected as the

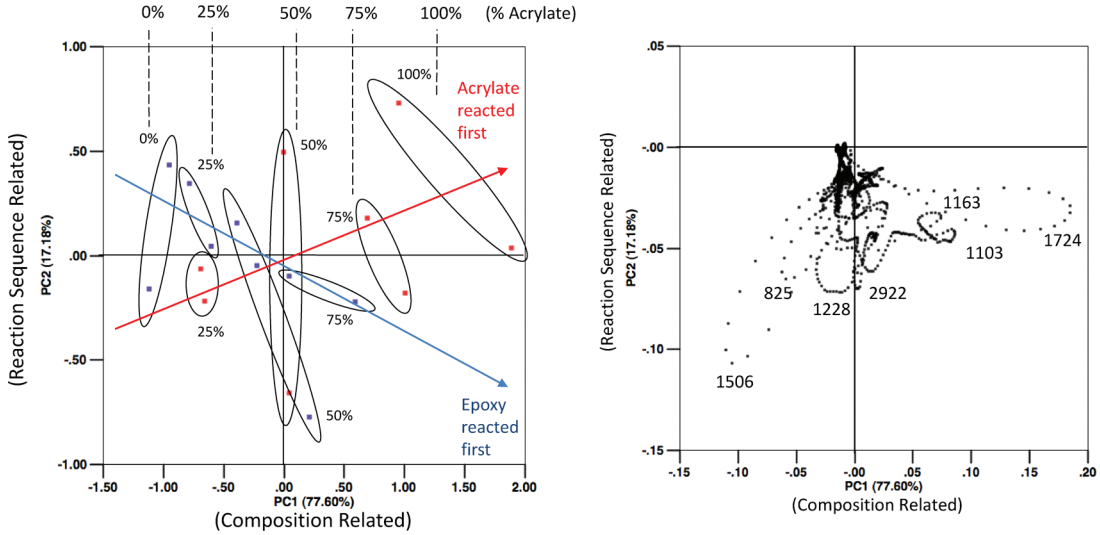

Figure 5. (a) Scores plot of the FTIR spectra from Figure 3. PC1 is identified as capturing differences in the spectra because of composition, while PC2 captures differences because of changing polymerization sequence. (b) Loadings plot corresponding with the FTIR spectra. The numbers labeled are the wavenumbers from the FTIR spectra. Further interpretation of this figure is provided in Table 2, with the term "loop" referring to the continuous points starting and ending at the origin.

Table 2. Features from Loadings Plot (Figure 5b) and the Interpretation of These Features

feature	interpretation
PC1	PC1 increases with increasing acrylate
PC2	PC2 is related to polymerization sequence
length of peak loops, magnitude of PC	variance in intensity of peak between samples
trajectory	impact of composition vs polymerization sequence
width of loop	captures peak shift between samples
asymmetry of loop	describes change in peak shape between samples
wavenumber sequence in loop	direction the peaks shift relative to wavenumber

polymerization was driven to completion and these reactive bonds should be completely consumed or formed in the resulting polymers. The only expected exception to this would be if one of the polymerizations restricted the complete reaction of the other monomer resulting in residual monomer, although that was not found to be the case for these samples.

The important wavenumbers from loop apexes from the loadings plot are equally divided in importance between PC1 (composition), PC2 (polymerization sequence), or both. An example is the loop apexes at 1508 cm^{-1} and 829 cm^{-1}, which together correspond to para-substituted aromatic C═C bonds. The importance of this region to both PC1 and PC2 on the loadings plot suggests there may be differences in the samples' spectra related to differences in aromatic ring bonding energies, which are most likely due to configurations or constrain of the polymer,[32] as the chemistry of the aromatic ring is not affected by polymerization or polymerization sequence.

Table 3. Wavenumbers Identified from FTIR Spectra and from PCA Loadings Plot with Associated Bond, Associated Monomer, Whether the Bond Changed during Polymerization, and Whether the Peak Was Identified from PCA

wavenumber, cm^{-1}	bond	monomer	reactive	loadings plot
807	CH2= twist	epoxy		
829	para-substituted aromatic	epoxy		both
865	epoxide	epoxy	yes	
916	epoxide	epoxy	yes	
1103	C−O or C−C	epoxy		PC2
1163	C−X region	Both		PC1
1228	C−O or C−C	epoxy		PC2
1407	CH═CH2	Acrylate	yes	
1508	aromatic C═C, CH3 bend	epoxy		both
1606	aromatic C═C	epoxy		
1635	acrylate C═C	Acrylate	yes	
1726	C═O stretch	Acrylate		PC1
2922	sp^3 CH	Both		PC2

The changes in bond energies at 1228 cm^{-1} (C−O in epoxy) and 2922 cm^{-1} (CH in both) with reaction sequence indicate that the reaction sequence affects hydrogen bonding. These differences in molecular ordering with polymerization sequence as indicated by changes in the FTIR spectra have previously been demonstrated to translate to differences in physical properties and morphology.[6] It is significant that differences in the FTIR spectra that can be attributed to differences in polymerization sequence can be correlated to changes in physical properties.

The impact of this work is that we are able to identify the effects resulting from changing polymerization sequence as compared to varying the composition by analyzing the FTIR spectra of the samples. Another interesting take-away message is that if only the reactive peaks that are typically considered are analyzed, important

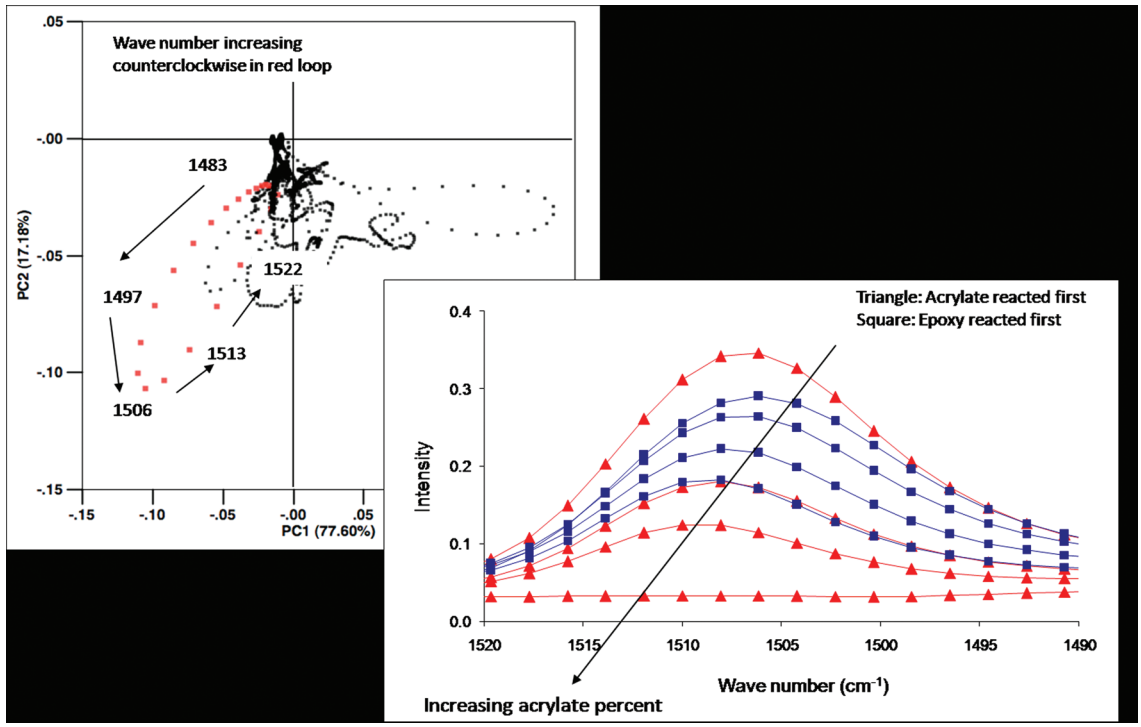

Figure 6. Demonstration of how the symmetry and width of a loop can be used to understand the relationship between the various spectra using one curve instead of many curves. Each point in the PCA loadings plot represents the spectra of all of the samples at the respective wavenumber. The loadings plot not only condenses the information on peak shift, peak intensity change, and differences between chemistries and polymerization sequences, but also ranks the peaks in terms of information contained.

information is missed. When reviewing the input data, clearly differentiating the changes in spectra because of changing composition or polymerization sequence is difficult without the use of data mining. We were able to quantify such a relationship between composition and polymerization sequence with FTIR spectra by studying the trajectory of a loop on a PCA loadings plot. In effect, a tool for the visualization of numerous spectra has been developed which quickly identifies spectral bands, which change most between samples.

5. Conclusions

We have analyzed FTIR spectra and rheological and tensile properties of acrylate/epoxy IPNs. Using a multivariate analysis, we were able to identify the wavenumber bands that are most impacted by the composition or polymerization sequence of the samples and to quantify this change. By visualizing the spectra in a manner based on the variance between the samples, we could identify which wavenumber regions are most impacted by the different effects (composition or polymerization sequence) and correlate this effect to related molecular bonding. We identified hydrogen bonds and aromatic ring bond energies as being largely impacted by changing the order of polymerization. By identifying the molecular bonding and physical properties affected by composition and polymerization sequence, the impact of processing on properties can be described and the responsible molecular bonding identified. This work builds a linkage between structure, chemistry, processing, and properties of IPN samples and builds a framework for rationally designing IPNs.

Acknowledgment. The author acknowledges support from 3M Corporation, the Institute of Combinatorial Discovery at Iowa State University, the National Science Foundation International Materials Institute Program for the Combinatorial Sciences and Materials Informatics Collaboratory (CoSMIC-IMI), Grant DMR--08-33853; the Office of Naval Research MURI program for Novel Vaccines: Targeting and Exploiting the Bacterial Quorum Sensing Pathway, award number N00014-06-1-1176.

Appendix

Definition of Physical Properties

Abbreviation	Description
x_a	Acrylate fraction
E	Young's modulus
e	Strain at peak (%)
s	Stress at peak (MPa)
H	Hardness
M	Mass of sample for mDSC from tensile specimens
T_{gI}	Tensile sample initial T_g during ramp up, °C
T_{gF}	Tensile sample final T_g during ramp down, °C
ΔH_R	Tensile sample residual nonreversible reaction heat, J/g
T_I	Tensile sample reaction initiation temperature, °C
T_P	Tensile sample reaction peak temperature, °C
dh/dt_P	Tensile sample peak reaction rate, W/g
α_E	Tensile sample epoxy conversion from residual reaction heat
IE 914	Tensile sample IR absorbance of epoxy at 914 cm
IE 1606	Tensile sample IR absorbance at 1606 cm^{-1}. This is a reference band for epoxy.
IE 1508	Tensile sample IR absorbance at 1508 cm^{-1}. This is a reference band for epoxy.
IA	Tensile sample absorbance of the acrylate peak at 1635 cm^{-1}
aE 1606	Tensile sample conversion of epoxy using absorbance at 1606 cm^{-1} as a reference.
aE 1508	Tensile sample conversion of epoxy using absorbance at 1508 cm^{-1} as a reference.
aA	Tensile sample acrylate conversion based on absorbance at 1635 cm^{-1}.
L	Thickness of the tensile sample at the dogbone neck (mm)
W	Width of the tensile sample at the dogbone neck (mm)
T_g	Glass transition temperature determined by rheometry (°C)
tan δ	tan delta
G′	Storage modulus determined by rheometry
G″	Loss modulus determined by rheometry
mRh	Mass of the sample used for mDSC taken from the rheology sample (mg)
T_{gI} Rh	Rheology sample initial T_g during ramp up, °C
T_{gF} Rh	Rheology sample final T_g during ramp down, °C
ΔH_R Rh	Rheology sample residual nonreversible reaction heat, J/g
T_I Rh	Rheology sample reaction initiation temperature, °C
T_P Rh	Rheology sample reaction peak temperature, °C
dh/dtP Rh	Rheology sample peak reaction rate
aE Rh	Rheology sample epoxy conversion from residual reaction heat
IE914 Rh	Rheology sample IR absorbance of epoxy at 914 cm^{-1}
IE 1606 Rh	Rheology sample IR absorbance at 1606 cm^{-1}. This is a reference band for epoxy.
IE 1508 Rh	Rheology sample IR absorbance at 1508 cm^{-1}. This is a reference band for epoxy.
IA Rh	Tensile sample absorbance of the acrylate peak at 1635 cm^{-1}
aE 1606 Rh	Rheology sample conversion of epoxy using absorbance at 1606 cm^{-1} as a reference
aE 1508 Rh	Rheology sample conversion of epoxy using absorbance at 1508 cm^{-1} as a reference
aA Rh	Rheology sample acrylate conversion based on absorbance at 1635 cm^{-1}

References and Notes

(1) Rajan, K. *Annu. Rev. Mater. Res.* **2008**, *38*, 299–322.
(2) Broderick, S.; Suh, C.; Nowers, J.; Vogel, B.; Mallapragada, S.; Narasimhan, B.; Rajan, K. *J. Met., Mater. Miner.* **2008**, *60*, 56–59.
(3) Rajan, K. *Mater. Today* **2005**, *8* (10), 38–45.
(4) Nowers, J. R.; Broderick, S. R.; Rajan, K.; Narasimhan, B. *Macromol. Rapid Commun.* **2007**, *28* (8), 972–976.
(5) Suh, C.; Rajan, K.; Vogel, B. M.; Narasimhan, B.; Mallapragada, S. K. Informatics methods for combinatorial materials science. In *Combinatorial Materials Science*; Wiley-Interscience: Hoboken, NJ, 2007.
(6) Nowers, J. R.; Costanzo, J. A.; Narasimhan, B. *J. Appl. Polym. Sci.* **2007**, *104* (2), 891–901.
(7) Frisch, H. L.; Du, Y.; Schulz, M. *Interpenetrating polymer network (IPN) materials, in Polymer Networks, Principles of their Formation, Structure and Properties*; Blackie Academic & Professional: London, 1998.
(8) Sperling, L. H. Interpenetrating Polymer Networks: An Overview. In *Interpenetrating Polymer Networds*; American Chemical Sociey: Washington, DC, 1994.
(9) Yoo, S. H.; Cohen, C.; Hui, C.-Y. *Polymer* **2006**, *47* (17), 6226–6235.
(10) Dean, K.; Cook, W. D. *Macromolecules* **2002**, *35* (21), 7942–7954.
(11) Nowers, J. R.; Narasimhan, B. *Polymer* **2006**, *47* (4), 1108–1118.
(12) Daffertshofer, A.; Lamoth, C. J. C.; Meijer, O. G.; Beek, P. J. *Clin. Biomech.* **2004**, *19* (4), 415–428.

(13) Berthiaux, H.; Mosorov, V.; Tomczak, L.; Gatumel, C.; Demeyre, J. F. *Chem. Eng. Process.* **2006**, *45* (5), 397–403.
(14) Ericksson, L.; Johansson, E.; Kettaneh-Wold, N.; Wold, S. *Multi- and Megavariate Data Analysis: Principles, Applications*;. Umetrics Ab: Umea, 2001.
(15) Hansen, L. K.; Larsen, J.; Nielsen, F. A.; Strother, S. C.; Rostrup, E.; Savoy, R.; Lange, N.; Sidtis, J.; Svarer, C.; Paulson, O. B. *NeuroImage* **1999**, *9* (5), 534–544.
(16) Lehmus, K.; Karppinen, M. *J. Solid State Chem.* **2001**, *162* (1), 1–9.
(17) Suh, C.; Rajan, K. *Appl. Surf. Sci.* **2004**, *223* (1−3), 148–158.
(18) Jóhannesson, G. H.; Bligaard, T.; Ruban, A. V.; Skriver, H. L.; Jacobsen, K. W.; Nørskov, J. K. *Phys. Rev. Lett.* **2002**, *88* (25), 255506.
(19) Mohn, C. E.; Kob, W. *Comput. Mater. Sci.* **2009**, *45*, 111–117.
(20) Fischer, C. C.; Tibbetts, K. J.; Morgan, D.; Ceder, G. *Nat. Mater.* **2006**, *5* (8), 641–646.
(21) Trimarchi, G.; Zunger, A. *Phys. Rev. B: Condens. Matter Mater. Phys.* **2007**, *75* (10), 104113–104118.
(22) Sluiter, M. H. F. *Acta Materialia* **2007**, *55* (11), 3707−3718.
(23) Chen, J.; Yang, T.; Luo, Q.; Breneman, C. M.; Cramer, S. M. *React. Funct. Polym.* **2007**, *67* (12), 1561–1569.
(24) Navarro-Villoslada, F.; Vicente, B. S.; Moreno-Bondi, M. C. *Anal. Chim. Acta* **2004**, *504* (1), 149–162.
(25) Qiao, R.; Catherine Brinson, L. *Compos. Sci. Technol.* **2009**, *69* (3−4), 491–499.
(26) Smentkowski, V. S.; Duong, H. M.; Tamaki, R.; Keenan, M. R.; Ohlhausen, J. A. T.; Kotula, P. G. *Appl. Surf. Sci.* **2006**, *253* (2), 1015–1022.
(27) Song, M.; Breneman, C. M.; Sukumar, N. *Bioorg. Med. Chem.* **2004**, *12* (2), 489–499.
(28) Alsberg, B. K.; Winson, M. K.; Kell, D. B. *Chemom. Intell. Lab. Syst.* **1997**, *36* (2), 95–109.
(29) Broderick, S. R.; Aourag, H.; Rajan, K. *Stat. Anal. Data Min.* **2009**, *1*, 353–360.
(30) Pate, M. E.; Turner, M. K.; Thornhill, N. F.; Titchener-Hooker, N. J. *Biotechnol. Prog.* **2004**, *20* (1), 215–222.
(31) Westad, F.; Martens, H. *Chemom. Intell. Lab. Syst.* **1999**, *45* (1−2), 361–370.
(32) Koenig, J. L. *Spectroscopy of Polymers*, 2nd ed.; Elsevier: New York, 1999.

CC900145D